DE GRUYTER Open Physics 2024; 22: 20240004

Research Article

Arezu Jahanshir*, Ekwevugbe Omugbe, Joseph Ngene Aniezi, Ifeanyi Jude Njoku, Clement Atachegbe Onate, Edwin Samson Eyube, Samuel Olugbade Ogundeji, Chinonso Mbamara, Raphael Mmaduka Obodo, and Michael Chukwudi Onyeaju

Heavy mesons mass spectroscopy under a spin-dependent Cornell potential within the framework of the spinless Salpeter equation

https://doi.org/10.1515/phys-2024-0004
received January 10, 2024; accepted March 07, 2024

Abstract: The energy bound-state solutions of the spinless Salpeter equation (SSE) have been obtained under a spin-dependent Cornell potential function *via* the Wentzel–Kramers–Brillouin approximation. The energy levels were applied to predict the mass spectra for the charmonium, bottomonium, and bottom-charmed mesons. The relativistic corrections for the angular momentum quantum number $l > 0$, total angular momentum quantum numbers $j = l$, $j = l \pm 1$, and the radial quantum numbers $n = 1$–4 improve the mass spectra. The results agree fairly with experimental data and theoretic results reported in existing works, where the authors utilized different forms of the inter-quark potentials and methods. The deviation of the obtained masses for the charmonium and bottomonium from the observed data yields a total percentage error of 3.32 and 1.11%, respectively. The results indicate that the accuracy of the masses is correlated with the magnitude of masses for the charm and bottom quarks. The SSE together with the phenomenological spin-dependent Cornell potential provides an adequate account of the mass spectroscopy for the heavy mesons and may be used to predict other spectroscopic parameters.

Keywords: meson spectroscopy, spin–orbit coupling, Cornell potential, Salpeter equation

*** Corresponding author: Arezu Jahanshir,** Department of Physics and Engineering Sciences, Buein Zahra Technical University, Buein Zahra, Iran, e-mail: jahanshir@bzte.ac.ir
Ekwevugbe Omugbe, Joseph Ngene Aniezi, Chinonso Mbamara, Raphael Mmaduka Obodo: Department of Physics, University of Agriculture and Environmental Sciences, Umuagwo, P.M.B. 1038, Imo State, Nigeria
Ifeanyi Jude Njoku: Department of Physics, Federal University of Technology Owerri, P.M.B.1526, Ihiagwa, Owerri, Imo State, Nigeria
Clement Atachegbe Onate: Department of Physical Sciences, Bowen University, Iwo, Osun State, Nigeria
Edwin Samson Eyube: Department of Physics, Faculty of Physical Sciences, Modibbo Adama University, P.M.B. 2076, Yola, Adamawa State, Nigeria
Samuel Olugbade Ogundeji: Department of Physics and Astronomy, Iowa state University, Ames, United States of America
Michael Chukwudi Onyeaju: Theoretical Physics Group, Department of Physics, University of Port Harcourt, Choba, Rivers State, Nigeria

1 Introduction

The discovery of the electron by Thomson [1] in 1897 and the nucleus by Rutherford [2] in 1911 gave a fairly complete picture of the atomic structure. However, decades after these discoveries, several other elementary particles have been discovered with the aid of modern equipment such as particle colliders, detectors, and accelerators. These elementary particles that are the composite of much smaller particles are referred to as quarks. Quarks form the building blocks of matter, and their dynamical existence has been confirmed *via* experimental works on deep inelastic scattering of electrons and neutrons [3]. The standard model of elementary particles forms the basis for the understanding of particle physics, where the quarks have six flavors, namely, the up (u), down (d), top (t), bottom (b), strange (s), and charm (c) quarks; six leptons such as the electron (e), muon (μ), tau (τ), and their respective neutrinos (ν_e, ν_μ, ν_τ); the gauge; and the Higgs bosons. The quarks and leptons interact *via* the unified electroweak forces and the strong quantum chromo-dynamics (QCD) force. The strong QCD force is responsible for the binding of quarks into protons and neutrons, while the interaction between the leptons is mediated by the electromagnetic force. The weak nuclear force is associated with particle decay.

The bound states of three quarks give rise to the baryons, while the quark–antiquark pairs constitute the mesons. Both the baryons and mesons are grouped into hadrons. The hadrons with ½ integer spin are fermions and obey the Fermi-Dirac statistics, while bosons possess spin 0, 1 and obey the Bose–Einstein statistics. The properties of these elementary particles have garnered research interest among particle physicists in recent years. These properties have been observed using heavy machinery [4], and some were predicted theoretically before their experimental discovery. In this regard, the bound-state solutions of the wave equations under the inter-quark potentials have been utilized to predict the mass spectroscopy and decay properties of the elementary particles. The most utilized potential energy is the Cornell potential, which is the combination of the Coulomb's energy and a linear function. The Coulomb's energy is responsible for the short-range gluon exchange interaction between a quark and its antiquark, while the linear function is in charge of quark confinement. The addition of spin components to the Cornell potential allows for relativistic corrections and results in the hyperfine splitting between the s-wave singlet and triplet states. The multiple triplet splitting occurs for any angular momentum quantum number $l > 0$.

Li *et al.* [5] predicted the charmonium ($c\bar{c}$) mass spectra using the coupled-channel model and the screened potential model in the mass region below 4 GeV. Their results agreed with the masses of the $c\bar{c}$ meson obtained with a quenched potential model and literature data [6]. Mutuk [7] investigated the mass spectra and decay constants of vector and pseudoscalar heavy-light mesons within the framework of the QCD sum rule and the quark model. The numerical results were in good agreement compared to observed data and other theoretical works. The charmonia spectra have been investigated using the non-relativistic quark model and matrix-Numerov method [8,9]. Chaturvedi and Rai [10], in a recent work, investigated the electromagnetic transitions, mass spectroscopy, and decay rates of the bottom-charm ($b\bar{c}$) meson within the context of the non-relativistic QCD. Several authors [11–28] have carried out extensive studies on the mesons bound-state solutions and applied them to obtain their spectroscopic parameters. The results in the references therein were compared to experimental data of the particle data group [29–31], and the results were predicted using different QCD-inspired potentials, phenomenological potentials, and theoretical methods.

In this work, we investigate the hyperfine mass spectra splitting of the heavy mesons within the framework of the semi-relativistic spinless Salpeter equation (SSE). Previously, the mass spectra of the heavy mesons have been obtained in previous studies [32,33] using the SSE without considering the spin components and relativistic corrections for the inter-quark potentials. The results in the references therein revealed that the semi-relativistic equation provides a satisfying account for the meson mass spectroscopy. Motivated by these facts, we report for the first time the approximate analytical and numerical mass spectra splitting of the heavy mesons under the SSE with a phenomenological spin-dependent Cornell potential *via* the Wentzel–Kramers–Brillouin (WKB) approximation.

In this study, we considered the interactions potential function given by

$$V(r) = V_{\mathrm{c}}(r) + V_{\mathrm{SS}}(r) + V_{\mathrm{LS}}(r) + V_{\mathrm{T}}(r), \tag{1}$$

where $V_{\mathrm{c}}(r)$ is the Cornell potential. The functions $V_{\mathrm{SS}}(r)$, $V_{\mathrm{LS}}(r)$, and $V_{\mathrm{T}}(r)$ are the spin–spin, spin–orbit, and tensor channels, respectively. The respective potential functions are represented as [22,24]

$$V_{\mathrm{c}}(r) = -\frac{4\alpha_s}{3r} + br, \tag{2}$$

$$V_{\mathrm{SS}}(r) = \frac{32\pi\alpha_s}{9m_q m_{\bar{q}}}\bar{\delta}_\sigma(r)\langle\bar{\boldsymbol{S}}\cdot\bar{\boldsymbol{S}}\rangle, \tag{3}$$

$$V_{\mathrm{LS}}(r) = \frac{1}{m_q m_{\bar{q}}}\left(\frac{2\alpha_s}{r^3} - \frac{b}{2r}\right)\langle\bar{\boldsymbol{L}}\cdot\bar{\boldsymbol{S}}\rangle, \tag{4}$$

$$V_{\mathrm{T}}(r) = \frac{4\alpha_s}{m_q m_{\bar{q}} r^3}\langle\bar{\boldsymbol{T}}\rangle, \tag{5}$$

where α_s, b, m_q, and $m_{\bar{q}}$ are the coupling constant, linear confinement parameter, the mass of quark, and its antiquark, respectively. In (3), the Dirac delta function has been used as a Gaussian function ($\bar{\delta}_\sigma(r) = (\sigma/\sqrt{\pi})^3 e^{-\sigma^2 r^2}$). The operators in Eqs. (3)–(5) are diagonal in $|j, l, s\rangle$ with the respective spin–spin ($\langle\bar{\boldsymbol{S}}\cdot\bar{\boldsymbol{S}}\rangle$) spin–orbit ($\bar{\boldsymbol{L}}\cdot\bar{\boldsymbol{S}}$) and tensor ($\bar{\boldsymbol{T}}$) matrix elements given by refs [22,24]

$$\langle\bar{\boldsymbol{S}}\cdot\bar{\boldsymbol{S}}\rangle = \frac{s(s+1)}{2} - \frac{3}{4}, \tag{6}$$

$$\langle\bar{\boldsymbol{L}}\cdot\bar{\boldsymbol{S}}\rangle = \frac{1}{2}(j(j+1) - l(l+1) - s(s+1)), \tag{7}$$

$$\langle n^3 l_j|\bar{\boldsymbol{T}}|n^3 l_j\rangle = -\frac{6(\langle\bar{\boldsymbol{L}}\cdot\bar{\boldsymbol{S}}\rangle)^2 + 3\langle\bar{\boldsymbol{L}}\cdot\bar{\boldsymbol{S}}\rangle - 2s(s+1)l(l+1)}{6(2l-1)(2l+3)}. \tag{8}$$

The notations s, l, and $j = l + s$ denote the spin number, orbital quantum number, and the total angular momentum quantum number, respectively. The spin–spin coupling gives rise to the s-wave ($l = 0$) hyperfine splitting between the triplet ($s = 1$) and singlet ($s = 0$) states. For $l > 0$, and $j = l \pm 1, j = l$, we have the multiplets splitting for the p, d, f, g, and h triplets quantum states. The n represents the principal quantum number. The spin-dependent potentials in (4) and (5) give the mass shifts and are obtained from leading-order perturbation theory [14,24]. The operator $\langle\bar{\boldsymbol{T}}\rangle$ can be described by the non-vanishing diagonal matrix element for $l > 0$ and correspond to the spin triplet states [21].

2 Energy spectrum of the SSE with spin-dependent Cornell potential *via* the WKB approximation

To obtain an approximate analytical solution, we truncate the Gaussian function to a harmonic function for $r \ll 1$ fm *via* a Taylor series expansion around $r = 0$. The Gaussian function can be expressed as $e^{-\sigma^2 r^2} \sim 1 - \sigma^2 r^2$. In the femtometer scale, this approximation is important for quark interactions [28].

Using this approximation, the potential in (1) can be simplified as

$$V(r) = -\frac{Q}{r} + br + \frac{N}{r^3} - Pr^2 + \Omega_s, \tag{9}$$

where

$$Q = \frac{4\alpha_s}{3} + \frac{b(\bar{\boldsymbol{L}}\cdot\bar{\boldsymbol{S}})}{2m_q m_{\bar{q}}}, \tag{10}$$

$$N = \frac{2\alpha_s(\bar{\boldsymbol{L}}\cdot\bar{\boldsymbol{S}})}{m_q m_{\bar{q}}} + \frac{4\alpha_s(\bar{\boldsymbol{T}})}{m_q m_{\bar{q}}}, \tag{11}$$

$$P = \sigma^2\Omega_s, \tag{12}$$

$$\Omega_s = \frac{16\pi\alpha_s}{9m_q m_{\bar{q}}}(\sigma/\sqrt{\pi})^3(s(s+1) - 1.5). \tag{13}$$

The spinless SSE equation for describing a two-body system is given as [34,35]

$$\left(\sum_{i=1,2}\sqrt{-\Delta + m_i^2} + V(r) - E_{nl}\right)\xi(r,\theta,\varphi) = 0, \quad \Delta = \nabla^2, \tag{14}$$

where

$$\xi(r,\theta,\varphi) = \psi_{nl}(r)Y_{lm}(\theta,\varphi). \tag{15}$$

The notations ∇^2, $V(r)$, E_{nl}, and $\xi(r,\theta,\varphi)$ represent the Laplacian, the potential function, total energy, and the total wave function, respectively.

For interaction between particles, the summation in Eq. (14) can further be expanded *via* Taylor series to order two:

$$\sum_{i=1,2}\sqrt{-\Delta + m_i^2} = m_1 + m_2 - \frac{\Delta}{2\mu} - \frac{\Delta^2}{8\eta^3}, \tag{16}$$

where

$$\mu = \frac{m_1 m_2}{m_1 + m_2}, \eta = \mu\left(\frac{m_1 m_2}{m_1 m_2 - 3\mu^2}\right)^{1/3}.$$

Eq. (14) can further be reduced to a Schrödinger-like equation [35]

$$\left(-\frac{1}{2\mu}\frac{d^2}{dr^2} + V(r) - E_{nl} - \frac{1}{2\tilde{m}}(V(r) - E_{nl})^2 + \frac{(l+1/2)^2}{2\mu r^2}\right)\psi_{nl}(r) = 0, \hbar = 1, \tilde{m} = \frac{\eta^3}{\mu^2}. \tag{17}$$

Eq. (17) can be written as a momentum eigenvalue equation

$$((\hat{\boldsymbol{P}})^2 + p_\mu^2(r))\psi_{nl}(r) = 0, \tag{18}$$

where $\hat{\boldsymbol{P}}$ is the radial momentum operator and $p_\mu(r)$ is the meson momentum eigenvalue given as

$$p_\mu(r) = \sqrt{2\mu\left(\frac{1}{2\tilde{m}}(V(r) - E_{nl})^2 - (V(r) - E_{nl}) - \frac{(l+1/2)^2}{2\mu r^2}\right)}. \tag{19}$$

To obtain the energy equation for the modeled potential, we employed the WKB energy quantization condition for two real turning points r_1 and r_2 *via* the integral equation:

$$\int_{r_1}^{r_2} p_\mu(r)\mathrm{d}r = \pi\left(n + \frac{1}{2}\right), \hbar = 1. \tag{20}$$

It is worth stating that we have added a Langer's correction [36] to the centrifugal potential using the transformation $l(l+1) \to (l+1/2)^2$. This correction in the WKB approximation admits the exact energy eigenvalues for soluble potentials and ensures that the wave function is well behaved near the origin.

Inserting the momentum into the WKB quantization integral in (20) with the potential energy given by (1), we obtained

$$\sqrt{2\mu}\int_{r_1}^{r_2}\sqrt{\frac{A}{r^6} - \frac{B}{r^4} + \frac{C}{r^3} + \frac{D}{r^2} - \frac{E}{r} + \Lambda r^4 - Fr^3 + Gr^2 + Hr + \mathrm{K}}\,\mathrm{d}r = \pi\left(n + \frac{1}{2}\right), \tag{21}$$

where

$A = \frac{N^2}{2\tilde{m}}$, $B = \frac{2QN}{2\tilde{m}}$, $C = \frac{2N\Omega_s - 2NE_{nl}}{2\tilde{m}} - N$, $D = \frac{Q^2 + 2Nb}{2\tilde{m}} - L$, $E = \frac{2Q\Omega_s + 2PN - 2QE_{nl}}{2\tilde{m}} - Q$, $F = \frac{2Pb}{2\tilde{m}}$, $G = \frac{b^2 - 2P\Omega_s + 2PE_{nl}}{2\tilde{m}} + P$, $H = \frac{2b\Omega_s + 2PQ - 2bE_{nl}}{2\tilde{m}} - b$, $\mathrm{K} = \frac{(E_{nl} - \Omega_s)^2 - 2Qb}{2\tilde{m}} + E_{nl} - \Omega_s$, $\Lambda = \frac{P^2}{2\tilde{m}}$, $L = \frac{(l+1/2)^2}{2\mu}$.

Using coordinate transformation $q = 1/r$, Eq. (21) reduces to

$$-\sqrt{2\mu}\int_{q_1}^{q_2}\sqrt{Aq^2 - B + \frac{C}{q} + \frac{D}{q^2} - \frac{E}{q^3} + \frac{\Lambda}{q^8} - \frac{F}{q^7} + \frac{G}{q^6} + \frac{H}{q^5} + \frac{\mathrm{K}}{q^4}}\,\mathrm{d}q = \pi\left(n + \frac{1}{2}\right). \tag{22}$$

To solve Eq. (22) analytically, the multiple turning points need to be reduced to two *via* a Pekeris-type approximation around $q = 0$. Let $q = y + \delta$ with $\delta(1/q)$ assumed to be the characteristic distance between the quark and anti-quark pairs. The inverse power terms can be obtained using the Taylor series expansion to the second order:

$$q^{-k} = \delta^{-k}\left(1 + \frac{y}{\delta}\right)^{-k} \sim \delta^{-k} - k\delta^{-k-1}y + \frac{k(k+1)}{2!}\delta^{-k-2}y^2 + O(y^3), \tag{23}$$

Table 1: Calculated parameters of interaction potential function

Parameters	**Potential free parameters**		
	Charmonium	**Bottomonium**	**Bc Meson**
Mass **(GeV)**	$m_c = m_{\bar{c}} = 1.530^{a}$	$m_b = m_{\bar{b}} = 5.250^{a}$	$m_c = 1.530$, $m_b = 5.250$
$\boldsymbol{\alpha_s}$	30.1602	27.7862	41.1745
$\boldsymbol{\delta}$ **(GeV)**	0.05846	0.0796	0.0796
$\boldsymbol{b}$ **(GeV²)**	0.1416	0.1702	0.2710
$\boldsymbol{\sigma}$ **(GeV)**	−0.1294	0.1356	0.1356

Note: [a]We choose the bottom and charm masses from the obtained range [29] $1.2 < m_c < 1.8\ \text{GeV}$ and $4.5 < m_b < 5.4\ \text{GeV}$.

Table 2: S and P-states mass spectrum of charmonium meson in GeV

State		**Present**	**[24]**	**[18]**	**[16]**	**[11]**	**[22]**	**Expt. [30]**
$\boldsymbol{n^{2s+1}L_j}$	$\boldsymbol{J^{PC}}$							
$J/\psi(1^3S_1)$	1^{--}	3.520	3.094	3.0413	3.096	3.126	3.0851	$3.097 \pm (6 \times 10^{-6})$
$\eta_c(1^1S_0)$	0^{-+}	3.293	2.989	3.1404	2.981	3.033	2.9904	2.984 ± 0.0004
$\psi(2^3S_1)$	1^{--}	3.902	3.681	3.7017	3.685	3.701	3.6821	$3.686 \pm (6 \times 10^{-5})$
$\eta_c(2^1S_0)$*	0^{-+}	3.638	3.602	3.6610	3.635	3.666	3.6465	$3.638 \pm (1.1 \times 10^{-3})$
$\psi(3^3S_1)$	1^{--}	4.194	4.129	4.0502	4.039	4.055	4.1002	4.039 ± 10^{-3}
$\eta_c(3^1S_0)$	0^{-+}	3.895	4.058	4.1347	3.989	4.158	4.0719	
$\psi(4^3S_1)$*	1^{--}	4.421	4.514	4.4185	4.427	4.415	4.4394	$4.421 \pm (4 \times 10^{-3})$
$\eta_c(4^1S_0)$	0^{-+}	4.091	4.448	4.4136	4.401	4.415	4.4209	
$\psi(5^3S_1)$	1^{--}	4.600	4.863	4.6591	4.837	4.585		$4.63 \pm (6 \times 10^{-3})$
$\eta_c(5^1S_0)$	0^{-+}	4.242	4.799	4.6618	4.811	4.607		
$\psi(6^3S_1)$	1^{--}	5.804	5.185	4.8801	5.167	4.733		
$\eta_c(6^1S_0)$	0^{-+}	5.175	5.124	4.8825	5.155	4.754		
$\chi_{c_1}(1^3P_1)$*	1^{++}	3.511	3.468	3.5036	3.511	3.487	3.5004	$3.511 \pm (5 \times 10^{-5})$
$\chi_{c_2}(1^3P_2)$	2^{++}	3.545	3.480	3.4888	3.555	3.522	3.5514	$3.556 \pm 7 \times 10^{-5}$
$\chi_{c_0}(1^3P_0)$	0^{++}	3.466	3.428	3.4137	3.413	3.407	3.3519	$3.415 \pm 3 \times 10^{-4}$
$h_c(1^1P_1)$	1^{+-}	3.298	3.470	3.5180	3.525	3.502	3.5146	$3.525 \pm (1.1 \times 10^{-4})$
$\chi_{c_1}(2^3P_1)$	1^{++}	3.895	3.938	3.8072	3.906	3.786	3.9335	$3.872 \pm (6 \times 10^{-5})$
$\chi_{c_2}(2^3P_2)$*	2^{++}	3.923	3.955	3.9151	3.949	3.905	3.9798	$3.923 \pm 1 \times 10^{-3}$
$\chi_{c_0}(2^3P_0)$	0^{++}	3.856	3.897	3.7646	3.870	3.899	3.8357	$3.922 \pm 1.8 \times 10^{-3}$
$h_c(2^1P_1)$	1^{+-}	3.642	3.943	3.8239	3.926	3.8210	3.9446	
$\chi_{c_1}(3^3P_1)$	1^{++}	4.188	4.338	4.1210	4.319	4.1230	4.3179	$4.147 \pm (3 \times 10^{-3})$
$\chi_{c_2}(3^3P_2)$	2^{++}	4.212	4.358	4.1514	4.354	4.144	4.3834	
$\chi_{c_0}(3^3P_0)$	0^{++}	4.155	4.296	4.0804	4.301	4.120	4.2167	
$h_c(3^1P_1)$	1^{+-}	3.899	4.344	4.1368	4.337	4.1640	4.3339	
$\chi_{c_1}(4^3P_1)$	1^{++}	4.416	4.696	4.4005	4.728	4.3730	4.6203	
$\chi_{c_2}(4^3P_2)$	2^{++}	4.436	4.718	4.4298	4.763	4.411	4.7367	
$\chi_{c_0}(4^3P_0)$	0^{++}	4.388	4.653	4.3621	4.698	4.362	4.5518	
$h_c(4^1P_1)$	1^{+-}	4.094	4.704	4.1455	4.744	4.4200	4.6395	

where

$q^{-1} = \frac{3}{\delta} - \frac{3q}{\delta^2} + \frac{3q^2}{\delta^3}$, $q^{-2} = \frac{6}{\delta^2} - \frac{8q}{\delta^3} + \frac{3q^2}{\delta^4}$, $q^{-3} = \frac{10}{\delta^3} - \frac{15q}{\delta^4} + \frac{6q^2}{\delta^5}$, $q^{-4} = \frac{15}{\delta^4} - \frac{24q}{\delta^5} + \frac{10q^2}{\delta^6}$, $q^{-5} = \frac{21}{\delta^5} - \frac{35q}{\delta^6} + \frac{15q^2}{\delta^7}$, $q^{-6} = \frac{28}{\delta^6} - \frac{48q}{\delta^7} + \frac{21q^2}{\delta^8}$, $q^{-7} = \frac{36}{\delta^7} - \frac{63q}{\delta^8} + \frac{28q^2}{\delta^9}$, $q^{-8} = \frac{45}{\delta^8} - \frac{80q}{\delta^9} + \frac{36q^2}{\delta^{10}}$.

Inserting the terms $q^{-k}(k = 1\text{–}8))$ into (22) with algebraic simplifications gives

$$-\sqrt{2\mu W}\int_{q_1}^{q_2}\sqrt{-q^2 + \aleph \mathrm{q} - T}\,\mathrm{d}q = \sqrt{2\mu W}\int_{q_2}^{q_1}\sqrt{(q_2 - q)(q - q_1)}\,\mathrm{d}q = \pi\left(n + \frac{1}{2}\right), \tag{24}$$

where

$$\aleph = \frac{1}{W}\left(\frac{63F}{\delta^8} - \frac{80\Lambda}{\delta^9} - \frac{48G}{\delta^7} - \frac{35H}{\delta^6} - \frac{24K}{\delta^5} + \frac{15E}{\delta^4} - \frac{8D}{\delta^3} - \frac{3C}{\delta^2}\right), \tag{25}$$

$$T = \frac{1}{W}\left(\frac{36F}{\delta^7} - \frac{45\Lambda}{\delta^8} - \frac{28G}{\delta^6} - \frac{21H}{\delta^5} - \frac{15K}{\delta^4} + \frac{10E}{\delta^3} - \frac{6D}{\delta^2} - \frac{3C}{\delta} + B\right), \tag{26}$$

$$W = \frac{28F}{\delta^9} - \frac{36\Lambda}{\delta^{10}} - \frac{21G}{\delta^8} - \frac{15H}{\delta^7} - \frac{10K}{\delta^6} + \frac{6E}{\delta^5} - \frac{3D}{\delta^4} - \frac{3C}{\delta^3} - A. \tag{27}$$

The turning points (q_1, q_2) in (24) are obtained by solving the $\sqrt{-q^2 + \aleph \mathrm{q} - T} = 0$, which is a requirement in the WKB approximation for the momentum to vanish at the classical turning points:

Table 3: D, F, and G-states mass spectrum of charmonium meson in GeV

State $n^{2s+1}L_j$	J^{PC}	Present	[24]	[18]	[16]	[11]	[22]	Expt. [30]
$\psi_2(1^3D_2)$	2^{--}	3.520	3.772	3.46047	3.795	3.3480	3.8077	
$\psi_3(1^3D_3)$	3^{--}	3.575	3.755	3.51402	3.813	3.307	3.8146	
$\psi_1(1^3D_1)$	1^{--}	3.461	3.775	3.40228	3.783	3.374	3.7853	$3.774 \pm 4 \times 10^{-4}$
$\eta_{c_2}(1^1D_2)$	2^{-+}	3.306	3.765	3.47795	3.807	3.3760	3.8073	
$\psi_2(2^3D_2)$	2^{--}	3.902	4.188	3.81161	4.190	3.8010	4.1737	$3.824 \pm (5 \times 10^{-4})$
$\psi_3(2^3D_3)$	3^{--}	3.949	4.176	3.86300	4.220	3.797	4.1829	
$\psi_1(2^3D_1)$	1^{--}	3.852	4.188	3.75606	4.150	3.800	4.1504	
$\eta_{c_2}(2^1D_2)$	2^{-+}	3.649	4.182	3.82825	4.196	3.8360	4.1737	
$\psi_2(3^3D_2)$	2^{--}	4.195	4.557	4.12502	4.544	4.1350	4.5588	
$\psi_3(3^3D_3)$	3^{--}	4.234	4.549	4.17431	4.574	4.163	4.5725	
$\psi_1(3^3D_1)$	1^{--}	4.152	4.555	4.07208	4.507	4.113	4.5258	
$\eta_{c_2}(3^1D_2)$	2^{-+}	3.905	4.553	4.14085	4.549	4.176	4.5597	
$\chi_{c_3}(1^3F_3)$	3^{++}	3.532	4.012	3.46746	4.068	3.375	4.0440	
$\chi_{c_4}(1^3F_4)$	4^{++}	3.609	4.036	3.54185	4.093	3.315	4.0374	
$\chi_{c_2}(1^3F_2)$	2^{++}	3.454	3.990	3.38961	4.041	3.403	4.0424	
$\eta_{c_3}(1^1F_3)$	3^{+-}	3.319	4.017	3.48494	4.071	3.403	4.0411	
$\chi_{c_3}(2^3F_3)$	3^{++}	3.913	4.396	3.81815	4.400	3.823	4.3744	
$\chi_{c_4}(2^3F_4)$	4^{++}	3.978	4.415	3.88949	4.434	3.814	4.3711	
$\chi_{c_2}(2^3F_2)$	2^{++}	3.846	4.378	3.74376	4.361	3.812	4.3699	
$\eta_{c_3}(2^1F_3)$	3^{+-}	3.660	4.400	3.83479	4.406	3.858	4.3723	
$\psi_{c_4}(1^3G_4)$	4^{--}	3.549			4.343		4.2506	
$\psi_{c_5}(1^3G_5)$	5^{--}	3.647			4.357		4.2369	
$\psi_{c_3}(1^3G_3)$	3^{--}	3.450			4.321		4.2582	
$\eta_{c_4}(1^1G_4)$	4^{-+}	3.336			4.345		4.2471	
Total error (χ)		3.32%	1.98%	1.64%	1.30%	1.33%	1.53%	

Table 4: S and P-states mass spectrum of bottomonium meson in GeV

State		Present	[17]	[16]	[18]	[11]	[14]	[24]	Expt. [30]
$n^{2s+1}L_j$	J^{PC}								
$\Upsilon(1^3S_1)$	1^{--}	9.906	9.465	9.460	9.49081	9.525	9.4600	9.4600	$9.460 \pm (2.6 \times 10^{-4})$
$\eta_b(1^1S_0)$	0^{-+}	9.916	9.402	9.398	9.43601	9.472	9.3900	9.4280	$9.399 \pm (2 \times 10^{-3})$
$\Upsilon(2^3S_1)$	1^{--}	10.240	10.003	10.023	10.01257	10.049	10.0150	9.9790	$10.023 \pm (3.1 \times 10^{-4})$
$\eta_b(2^1S_0)$	0^{-+}	10.251	9.976	9.990	9.99146	10.028	9.9900	9.9550	
$\Upsilon(3^3S_1)$	1^{--}	10.504	10.354	10.355	10.32775	10.371	10.3430	10.3590	$10.355 \pm (5 \times 10^{-4})$
$\eta_b(3^1S_0)$	0^{-+}	10.517	10.336	10.329	10.1386	10.360	10.3260	10.3380	
$\Upsilon(4^3S_1)$	1^{--}	10.715	10.635	10.586	10.5461	10.598	10.5970	10.6830	$10.579 \pm (1.2 \times 10^{-3})$
$\eta_b(4^1S_0)$	0^{-+}	10.729	10.623	10.573	10.3236	10.592	10.5840	10.6630	
$\Upsilon(5^3S_1)$	1^{--}	10.883	10.878	10.851	10.82628	10.870	10.8110	10.9750	$10.885 \pm (2.6 \times 10^{-3}) \pm (1.6 \times 10^{-3})$
$\eta_b(5^1S_0)$	0^{-+}	10.899	10.869	10.869	10.4977	10.790	10.8000	10.9560	
$\Upsilon(6^3S_1)$*	1^{--}	11.020	11.102	11.061	10.97061	11.022	10.9970	11.2430	$11.020 \pm (4 \times 10^{-3})$
$\eta_b(6^1S_0)$	0^{-+}	11.036	11.097	11.088	10.6615	10.961	10.9880	11.2260	11.014 [17]
$\chi_{b_1}(1^3P_1)$	1^{++}	9.906	9.876	9.892	9.87371	9.875	9.9030	9.8190	$9.893 \pm (2.6 \times 10^{-4}) \pm (3.1 \times 10^{-4})$
$\chi_{b_2}(1^3P_2)$*	2^{++}	9.912	9.897	9.912	9.89083	9.903	9.921	9.825	$9.912 \pm (2.6 \times 10^{-4}) \pm (3.1 \times 10^{-4})$
$\chi_{b_0}(1^3P_0)$	0^{++}	9.898	9.847	9.859	9.8432	9.840	9.864	9.806	$9.859 \pm (4.2 \times 10^{-4}) \pm (3.1 \times 10^{-4})$
$h_b(1^1P_1)$	1^{+-}	9.918	9.882	9.900	9.87919	9.884	9.9090	9.8210	$9.899 \pm (8 \times 10^{-4})$
$\chi_{b_1}(2^3P_1)$	1^{++}	10.240	10.246	10.255	10.21695	10.229	10.249	10.2170	$10.255 \pm (2.2 \times 10^{-4}) \pm (5 \times 10^{-4})$
$\chi_{b_2}(2^3P_2)$	2^{++}	10.245	10.261	10.268	10.22961	10.254	10.246	10.224	$10.269 \pm (2.2 \times 10^{-4}) \pm (5 \times 10^{-4})$
$\chi_{b_0}(2^3P_0)$*	0^{++}	10.233	10.226	10.233	10.19625	10.202	10.220	10.205	$10.233 \pm (4 \times 10^{-4}) \pm (5 \times 10^{-4})$
$h_b(2^1P_1)$	1^{+-}	10.254	10.250	10.260	10.22153	10.237	10.254	10.220	$10.260 \pm (1.2 \times 10^{-3})$
$\chi_{b_1}(3^3P_1)$	1^{++}	10.504	10.538	10.541	10.1378	10.339	10.515	10.553	$10.514 \pm (7 \times 10^{-4})$
$\chi_{b_2}(3^3P_2)$	2^{++}	10.509	10.550	10.550	10.1405	10.406	10.528	10.560	$10.524 \pm (8 \times 10^{-4})$
$\chi_{b_0}(3^3P_0)$	0^{++}	10.498	10.522	10.521	10.1342	10.299	10.490	10.540	10.500 [17]
$h_b(3^1P_1)$*	1^{+-}	10.519	10.541	10.544	4.14695	10.362	10.5190	10.556	10.519 [17]
$\chi_{b_1}(4^3P_1)$	1^{++}	10.715	10.788	10.802	10.3229	10.571		10.853	
$\chi_{b_2}(4^3P_2)$	2^{++}	10.719	10.798	10.812	10.3255	10.637		10.860	
$\chi_{b_0}(4^3P_0)$	0^{++}	10.710	10.775	10.781	10.3193	10.532		10.840	
$h_b(4^1P_1)$	1^{+-}	10.731	10.790	10.804	10.3242	10.594		10.855	

$$q_1 = \frac{\aleph}{2} - \frac{1}{2}\sqrt{\aleph^2 - 4T}, \tag{28}$$

$$q_2 = \frac{\aleph}{2} + \frac{1}{2}\sqrt{\aleph^2 - 4T}. \tag{29}$$

Solving (24), we obtained

$$\int_{q_2}^{q_1} \sqrt{(q_2 - q)(q - q_1)}\,\mathrm{d}q = \frac{\pi}{8}(q_1 - q_2)^2. \tag{30}$$

Comparing Eqs. (24) and (30), the condition for the energy-level equation is obtained as

$$\frac{\aleph^2}{4} - T = \sqrt{\frac{2}{\mu W}}\left(n + \frac{1}{2}\right). \tag{31}$$

The mass spectra are obtained from the relation between the quark masses and the energy eigenvalue:

$$M_{nl} = m_q + m_{\bar{q}} + E_{nl}. \tag{32}$$

3 Numerical results and discussion

The energy bound-state solution of the SSE under a spin-dependent Cornell potential has been obtained *via* the semi-classical WKB approximation method. The potential parameters (α_s, b, δ, σ) were obtained by fitting the obtained

Table 5: D, F, and G-states mass spectrum of bottomonium meson in GeV

$n^{2s+1}L_j$	J^{PC}	Present	[17]	[16]	[18]	[11]	[14]	[24]	Expt. [30]
$\Upsilon_2(1^3D_2)$	2^{--}	9.911	10.147	10.161	10.1126	10.096	10.153	10.075	$10.164 \pm (1.4 \times 10^{-3})$
$\Upsilon_3(1^3D_3)$	3^{--}	9.921	10.155	10.166	9.73855	9.849	10.157	10.073	10.172 [17]
$\Upsilon_1(1^3D_1)$	1^{--}	9.900	10.138	10.154	9.72905	9.666	10.146	10.074	10.155 [17]
$\eta_{b_2}(1^1D_2)$	2^{-+}	9.923	10.148	10.163	9.7355	9.767	10.153	10.074	10.165 [17]
$\Upsilon_2(2^3D_2)$	2^{--}	10.244	10.449	10.443	9.94259	10.071	10.432	10.424	
$\Upsilon_3(2^3D_3)$	3^{--}	10.253	10.455	10.449	9.94704	10.175	10.436	10.423	
$\Upsilon_1(2^3D_1)$	1^{--}	10.235	10.441	10.435	9.93775	9.996	10.425	10.423	
$\eta_{b_2}(2^1D_2)$	2^{-+}	10.258	10.450	10.445	9.94405	10.093	10.432	10.424	
$\Upsilon_2(3^3D_2)$	2^{--}	10.508	10.705	10.711	10.1391	10.345		10.733	
$\Upsilon_3(3^3D_3)$	3^{--}	10.516	10.711	10.717	10.1435	10.446		10.733	
$\Upsilon_1(3^3D_1)$	1^{--}	10.501	10.698	10.704	10.1344	10.272		10.731	
$\eta_{b_2}(3^1D_2)$	2^{-+}	10.523	10.706	10.713	10.1405	10.368		10.733	
$\chi_{b_3}(1^3F_3)$	3^{++}	9.918	10.355	10.346	9.7361	9.754	10.340	10.287	
$\chi_{b_4}(1^3F_4)$	4^{++}	9.932	10.358	10.349	9.74242	9.896	10.340	10.291	
$\chi_{b_2}(1^3F_2)$	2^{++}	9.904	10.350	10.343	9.72948	9.642	10.338	10.283	
$\eta_{b_3}(1^1F_3)$	3^{+-}	9.931	10.355	10.347	9.73759	9.778	10.339	10.288	
$\chi_{b_3}(2^3F_3)$	3^{++}	10.251	10.619	10.614	9.94462	10.081		10.607	
$\chi_{b_4}(2^3F_4)$	4^{++}	10.263	10.622	10.617	9.9508	10.219		10.609	
$\chi_{b_2}(2^3F_2)$	2^{++}	10.239	10.615	10.610	9.93815	9.971		10.604	
$\eta_{b_3}(2^1F_3)$	3^{+-}	10.265	10.619	10.615	9.94608	10.104		10.607	
$\Upsilon_4(1^3G_4)$	4^{--}	9.929	10.531	10.512					
$\Upsilon_5(1^3G_5)$	5^{--}	9.946	10.532	10.514					
$\Upsilon_3(1^3G_3)$	3^{--}	9.911	10.529	10.511					
$\eta_{b_4}(1^1G_4)$	4^{-+}	9.941	10.530	10.513					
Total error (χ)		1.11%	0.20%	0.11%	3.85%	0.96%	0.13%	0.66%	

mass spectra with the corresponding experimental masses of the particle data group in Tables 2–5. We present the parameters in Table 1. The quantum states in the asterisk correspond to the points where the potential parameters are fitted using (32). To check for accuracy, the potential parameters were obtained for random quantum numbers for the s-wave singlet and triplet states and also the hyperfine triplet states ($l > 0, j \geq 0$) where we choose the parameters that reproduce minimum total errors. Also, to obtain potential parameters for the bottom-charmed meson, we assumed a constant characteristic distance (δ) and spin-dependent constant (σ) due to the limited availability of experimental data. For the bottomonium and charmonium mesons, we solved four polynomial equations simultaneously with the help of Maple software, while two non-linear equations were solved for the bottom-charmed meson to obtain the parameters α_s and b. The variation of the potential function with distance for the heavy mesons is plotted in Figure 1(a–c). The potential curves for the triplet and singlet states account for linear confinement and short-range gluon exchange between the quark–antiquark pairs. The Coulomb part of the potential in the absence of tensor and spin orbit components dominates at short distances, whereas the linear component is prominent at large distances.

The total errors are obtained using the following formula:

$$\chi = \frac{100}{Z} \sum_{i=1}^{Z} \left| \frac{M_{nl}^{\mathrm{exp}} - M_{nl}^{\mathrm{theo}}}{M_{nl}^{\mathrm{exp}}} \right|, \tag{33}$$

where Z, M_{nl}^{exp}, and M_{nl}^{theo} are the respective number of experimental data points, experimental masses, and theoretically obtained masses. In Table 2, the mass spectra of charmonium for the s-wave increase as the quantum number increases with the singlet states bounded below the triplet states. The $J/\psi(1^3S_1)$ and $\eta_c(1^1S_0)$ are higher than the experimentally determined values. However, the other s-wave masses are in agreement with the experimental masses [30] and the masses obtained using other interquark potential functions and methods reported in the existing literature [11,16,18,22,24]. In comparison with

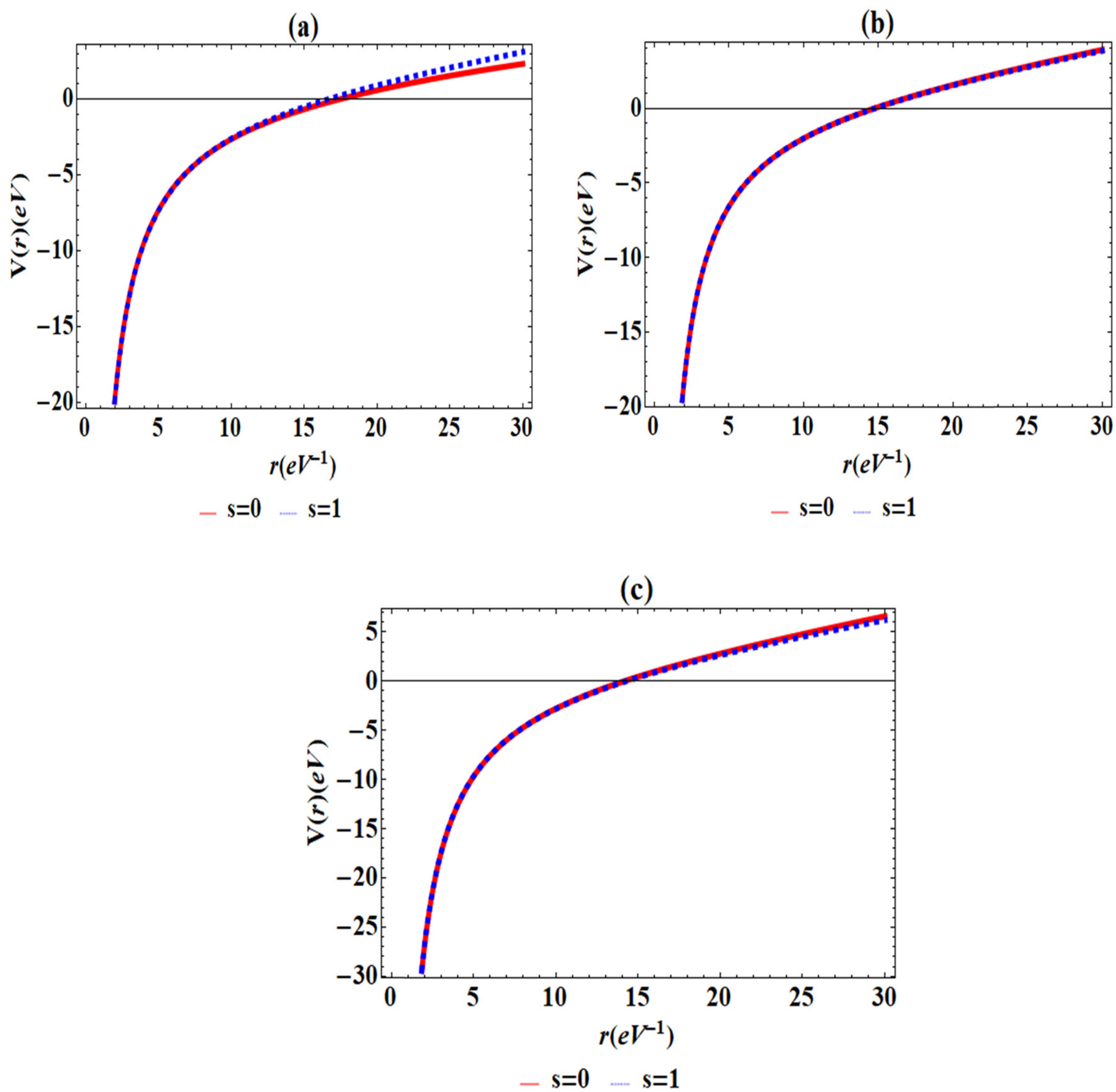

Figure 1: (a–c) Variation of potential function with distance: (a) charmonium, (b) bottomonium, and (c) bottom-charm mesons for spin numbers $s = 0$ and $s = 1$.

experimental data, the masses $\chi_{c_2}(1^3\mathrm{P}_2)$, $\chi_{c_0}(1^3\mathrm{P}_0)$, $\psi_1(1^3\mathrm{D}_1)$, and $\psi_2(2^3\mathrm{D}_2)$ with hyperfine splitting and relativistic corrections $l > 0$, $j = l, j = l \pm 1$ and $s = 1$ as shown in Tables 2 and 3 were found to be more accurate compared to the masses ($h_c(1^1\mathrm{P}_1)$, $\eta_{c_2}(1^1\mathrm{D}_2)$, and $\eta_{c_2}(2^1\mathrm{D}_2)$ for the quantum states ($l > 0$, $s = 0$, $j = l$). The charmonium masses for the s, p, d, and f states increase with the increase in the radial quantum number and were found to deviate from the experimental masses by a total error of 3.32%.

In Table 4, the bottomonium masses for the s and p-quantum states are presented. The low-lying quantum states masses are higher than the observed values. As the quantum number increases, the masses $\Upsilon(5^3\mathrm{S}_1)$ and $\eta_b(6^1\mathrm{S}_0)$ were found to be in good agreement compared to other works in the existing literature [11,14,16–18] and the masses of the particle data group [30]. The p-states masses were found to agree with the ones obtained earlier. However, the masses for d quantum states presented in Table 5 fairly compare with the observed masses [30]. Generally, the masses increase with the increase in the radial quantum number. Using Eq. (33), the bottomonium mass spectra deviation from experimental data yields a total percentage error of approximately 1.11%, which indicates an improvement over the results in the study by Mansour and Gamal [18] and comparable to the total percentage error of 0.96% in the study by Mansour and Gamal [11] and 0.66% in the study by Soni *et al.* [24]. It can be seen that the percentage error is higher for the charmonium meson due to its light reduced mass. In Tables 6 and 7, the masses obtained for the bottom-charmed mesons

Table 6: S and P states mass spectrum of bottom-charmed meson in GeV

State $n^{2s+1}L_j$	J^{PC}	Present	[16]	[11]	[24]	Expt. [31]
1^3S_1	1^{--}	6.225	6.333	6.313	6.321	
$(1^1S_0)^*$	0^{-+}	6.275	6.272	6.276	6.272	6.275
2^3S_1	1^{--}	6.783	6.882	6.867	6.900	
$(2^1S_0)^*$	0^{-+}	6.842	6.842	6.841	6.864	6.842
3^3S_1	1^{--}	7.216	7.258	7.308	7.338	
3^1S_0	0^{-+}	7.283	7.226	7.281	7.306	
4^3S_1	1^{--}	7.556	7.609	7.660	7.714	
4^1S_0	0^{-+}	7.631	7.585	7.634	7.684	
5^3S_1	1^{--}	7.826	7.947	7.941	8.054	
5^1S_0	0^{-+}	7.907	7.928	7.917	8.025	
6^3S_1	1^{--}	8.042		8.168	8.368	
6^1S_0	0^{-+}	8.130		8.144	8.340	
1^3P_1	1^{++}	6.218	6.743	6.281	6.705	
1^3P_2	2^{++}	6.248	6.761	6.366	6.712	
1^3P_0	0^{++}	6.178	6.699	6.223	6.686	
1^1P_1	1^{+-}	6.280	6.750	6.290	6.706	
2^3P_1	1^{++}	6.777	7.134	6.836	7.165	
2^3P_2	2^{++}	6.803	7.157	6.917	7.173	
2^3P_0	0^{++}	6.743	7.146	6.782	7.146	
2^1P_1	1^{+-}	6.847	7.147	6.846	7.168	
3^3P_1	1^{++}	7.211	7.500	7.278	7.555	
3^3P_2	2^{++}	7.233	7.524	7.355	7.565	
3^3P_0	0^{++}	7.182	7.474	7.227	7.536	
3^1P_1	1^{+-}	7.287	7.510	7.287	7.559	
4^3P_1	1^{++}	7.552	7.844	7.631	7.905	
4^3P_2	2^{++}	7.571	7.867	7.704	7.915	
4^3P_0	0^{++}	7.527	7.817	7.583	7.885	
4^1P_1	1^{+-}	7.634	7.853	7.640	7.908	

increases with the increase in the radial quantum number and were found to be in good agreement with the results in previous studies [11,16,24]. It is important to state that the accuracy of the mass spectra is dependent on obtaining a good fit for the phenomenological potential function. This allows for the adjustment of the potential parameters such that the predictions correspond as good as possible to other theoretic works and observed data.

4 Conclusions

The energy bound-state solution of the SSE has been obtained under a spin-dependent Cornell potential energy function using the WKB approximation approach. The energy equation was then used to obtain the mass spectra for the heavy mesons. The mass spectra were found to be in good agreement with the ones obtained by other methods. The charmonium masses deviated from the experimental values with a total percentage error of 3.32%. Also, the bottomonium masses deviated by 1.11%, which indicates an improvement compared to the results in the study by Mansour Gamal [18] and comparable to the works reported in the existing literature [11,24]. The errors were found to reduce significantly for the bottomonium meson due to its heavier mass. The points at which the fitting was carried out may be responsible for the low accuracy of the masses for the low-lying quantum states. However, the SSE together with the phenomenological spin-dependent Cornell potential provides an adequate account of the mass spectroscopy for the heavy mesons and may be used to predict other spectroscopic parameters if the wave function can be obtained.

Table 7: D, F, and G-states mass spectrum of bottom-charmed meson in GeV

$n^{2s+1}L_j$	J^{PC}	Present	[16]	[11]	[24]
1^3D_2	2^{--}	6.228	7.025	6.299	6.997
1^3D_3	3^{--}	6.278	7.029	6.429	6.990
1^3D_1	1^{--}	6.177	7.021	6.200	6.998
1^1D_2	2^{-+}	6.291	7.026	6.308	6.994
2^3D_2	2^{--}	6.787	7.399	6.852	7.403
2^3D_3	3^{--}	6.829	7.405	6.975	7.399
2^3D_1	1^{--}	6.742	7.392	6.759	7.403
2^1D_2	2^{-+}	6.856	7.400	6.861	7.401
3^3D_2	2^{--}	7.220	7.741	7.29	7.764
3^3D_3	3^{--}	7.256	7.750	7.409	7.764
3^3D_1	1^{--}	7.181	7.732	7.205	7.762
3^1D_2	2^{-+}	7.296	7.743	7.302	7.762
1^3F_3	3^{++}	6.244	7.269	6.326	7.242
1^3F_4	4^{++}	6.312	7.277	6.501	7.244
1^3F_2	2^{++}	6.175	7.273	6.182	7.234
1^1F_3	3^{+-}	6.307	7.268	6.335	7.241
2^3F_3	3^{++}	6.801	7.616	6.876	7.615
2^3F_4	4^{++}	6.859	7.617	7.041	7.617
2^3F_2	2^{++}	6.740	7.618	6.741	7.607
2^1F_3	3^{+-}	6.870	7.615	6.885	7.614
1^3G_4	4^{--}	6.265	7.489		
1^3G_5	5^{--}	6.353	7.482		
1^3G_3	3^{--}	6.178	7.497		
1^1G_4	4^{-+}	6.328	7.487		

Funding information: The authors state no funding involved.

Author contributions: The authors confirm contribution to this article as follows: study conception and design: Arezu Jahanshir, Ekwevugbe Omugbe; data collection: Ekwevugbe Omugbe, Joseph Ngene Aniezi, Ifeanyi Jude Njoku, Clement Atachegbe Onate; analysis and interpretation of results: Ekwevugbe Omugbe, Edwin Samson Eyube, Samuel Olugbade Ogundeji, Chinonso Mbamara; draft manuscript preparation: Arezu Jahanshir, Ekwevugbe Omugbe, Raphael Mmaduka Obodo, Michael Chukwudi Onyeaju. All authors have accepted responsibility for the entire content of this manuscript and approved its submission.

Conflict of interest: The authors state no conflict of interest.

References

[1] Thomson JJ. Cathode rays. Phil Mag. 1897;44:293–16.
[2] Rutherford E. The scattering of α and β particles by matter and the structure of the atom. Phil Mag. 1911;21(125):669–88.
[3] Ryder LH. Quantum field theory. Cambridge: Cambridge University Press; 1985.
[4] Mann R. An introduction to particle physics and the standard model. Boca Raton: CRC Press; 2021.
[5] Li BQ, Meng C, Chao KT. Coupled-channel and screening effects in charmonium spectrum. Phys Rev D. 2009;80:014012.
[6] Pininnington MR, Wilson DJ. Decay channels and charmonium mass shifts. Phys Rev D. 2007;76:077502.
[7] Mutuk H. S-wave heavy quarkonium spectra: Mass, decays, and transitions. Adv High Energy Phys. 2018;2018:5961031.
[8] Ali MS, Yasser AM, Hassan GS, Moustakidis CC. Spectra of quark-antiquark bound states *via* two derived QCD potentials. Quant Phys Lett. 2016;5(1):7–14.
[9] Ali MS, Hassan GS, Abdelmonem AM, Elshamndy SK, Elmasry F, Yasser AM. The spectrum of charmed quarkonium in non-relativistic quark model using matrix Numerov's method. J Radiat Res Appl Sci. 2020;13(1):226–33.
[10] Chaturvedi R, Rai AK. B_c meson spectroscopy motivated by general features of pNRQCD. Eur Phys J A. 2022;58:228.
[11] Mansour H, Gamal A, Abolmahassen M. Spin splitting spectroscopy of heavy quark and antiquarks systems. Adv High Energy Phys. 2020;2020:1–11.
[12] Bhavsar T, Shah M, Vinodkumar PC. Status of quarkonia-like negative and positive parity states in a relativistic confinement scheme. Eur Phys J C. 2018;78:227.
[13] Kher V, Rai AK. Spectroscopy and decay properties of charmonium. Chin Phys C. 2018;42(8):083101.
[14] Deng WJ, Liu H, Gui LC, Zhong XH. Spectrum and electromagnetic transitions of bottomonium. Phys Rev D. 2017;95:074002.
[15] Gupta P, Mehrotra I. Study of heavy quarkonium with energy dependent potential. J Mod Phys. 2012;3:1530–36.
[16] Ebert D, Faustov RN, Galkin VO. Spectroscopy and Regge trajectories of heavy quarkonia and mesons. Eur Phys J C. 2011;71:1825.
[17] Godfrey S, Moats K. Bottomonium mesons and strategies for their observation. Phys Rev D. 2015;92:054034.
[18] Mansour H, Gamal A. Meson spectra using Nikiforov-Uvarov method. Result Phys. 2022;33:105203.
[19] Boroun GR, Abdolmalki H. Variational and exact solutions of the wavefunction at origin (WFO) for heavy quarkonium by using aglobal potential. Phys Scr. 2009;80:065003.
[20] Chen H, Zhang J, Dong YB, Shen ON. Heavy quarkonium spectra in a quark potential model. Chin Phys Lett. 2001;18(12):1558.
[21] Barnes T, Godfrey S, Swanson ES. Higher charmonia. Phys Rev D. 2005;72:054026.
[22] Cao L, Yang YC, Chen H. Charmonium States in QCD-inspired quark potential model using Gaussian expansion method. Few-Body Syst. 2012;53:327–42.
[23] Kher V, Chaturvedi R, Devlani N, Rai AK. Bottomonium spectroscopy using Coulomb plus linear (Cornell) potential. Eur Phys J Plus. 2022;137:357.
[24] Soni NR, Johi BR, Shah RP, Chauhan HR, Pandya JN. $Q\bar{Q}(Q \in \{b, c\})$ spectroscopy using the Cornell potential. Eur Phys J C. 2018;78:592.
[25] Maireche A. A new model to describe Quarkonium systems under modified Cornell potential at finite temperature in pNRQCD. Int J Phys Chem. 2022;88:1–16.
[26] Maireche A. The relativistic and nonrelativistic solutions for the modified unequal mixture of scalar and time-like vector Cornell potentials in the symmetries of noncommutative quantum mechanics. Jordan J Phys. 2021;14(1):59–70.
[27] Maireche A, Imane D. A new nonrelativistic investigation for spectra of heavy quarkonia with modified Cornell potential: Noncommutative three dimensional space and phase space solutions. J Nano- Electron Phys. 2016;8(3):03024.
[28] Omugbe E, Aniezi JN, Inyang EP, Njoku IJ, Onate CA, Eyube ES, et al. Non-relativistic mass spectra splitting of heavy mesons under the Cornell potential perturbed by Spin–Spin, Spin–Orbit and tensor components. Few Body Syst. 2023;64:66.
[29] Ansler C, Doser M, Antonelli M, Anser DM, Babu KS, Baer H, et al. Particle data group. Phys Lett B. 2008;667:010001.
[30] Workman RL, Burkert VD, Crede V, Klempt E, Thoma U, Tiator L, et al. Particle data group. ProgTheor Exp Phys. 2022;2022:083C01.
[31] Patrignani C, Agashe K, Aielli G, Amsler C, Antonelli M, Asner DM, et al. Particle data group. Chin Phys C. 2016;40:100001.
[32] Omugbe E, Osafile OE, Okon IB, Inyang EP, William ES, Jahanshir A. Any *l*-state energy of the spinless Salpeter equation under the Cornell potential by the WKB approximation method: An application to mass spectra of mesons. Few Body Syst. 2022;63:6.
[33] Fulcher LP, Chen Z, Yeong JC. Energies of quark-antiquark systems, the Cornell potential, and the spinless Salpeter equation. Phys Rev D. 1993;47(9):4122–32.
[34] Salpeter EE. Mass corrections to the fine structure of hydrogen-like atoms. Phys Rev. 1952;87(2):328–43.
[35] Zarrinkamar S. Quasi-exact solutions for generalised interquark interactions in a two-body semi-relativistic framework. Z Naturforsch. 2016;71(11):1027–30.
[36] Langer RE. On the connection formulas and the solutions of the wave equation. Phys Rev. 1937;51:669–76.